GEOLOGIC MAPPING OF THE PLANCK QUADRANGLE OF THE MOON (LQ-29). R.A. Yingst[1], F.C. Chuang[1], D.C. Berman[1], and S.C. Mest[1]; [1]Planetary Science Institute (1700 E. Fort Lowell, Suite 106, Tucson, AZ 85719; yingst@psi.edu).

Introduction: A new systematic lunar geologic mapping effort has endeavored to build on the success of earlier mapping programs by fully integrating disparate new datasets using Geographic Information Systems (GIS) software and bringing to bear the most current understanding of lunar geologic history [1, 2]. This new mapping effort began with the division of the Moon into 30 quadrangles and preliminary mapping of the Copernicus Quadrangle [3, 4]. As part of this effort, we present a 1:2,500,000-scale map of the Planck Quadrangle (LQ-29; 30-60°S, 120-180°E; **Figure 1**, in review). To the south, it borders the South Pole Quadrangle (LQ-30) [5]. The area was mapped previously at 1:5,000,000 scale by [6-8]. The western portion of the pre-Nectarian South Pole-Aitken (SPA) impact feature covers much of the quadrangle's area.

Data and Mapping Methods: The ~ 100 m/pixel Lunar Reconnaissance Orbiter Camera (LROC) Wide Angle Camera (WAC) global mosaic formed the basemap for our mapping. This dataset provides a 3x improvement in resolution over Lunar Orbiter images, along with global nadir coverage. Additionally, we used LRO Lunar Orbiter Laser Altimeter (LOLA) [9, 10] and LRO WAC DTMs [11] to characterize the topographic expression of the surface and understand processes in vertical cross-section. The gridded LOLA and WAC DTMs provide complete coverage of the lunar surface at a resolution of ~100 m/pixel, and represent the most refined spatial and vertical (~1 m/pixel) resolutions acquired for the Moon.

Morphological features were mapped using the WAC basemap, while Clementine multispectral data were utilized to extract compositional information; we examined the 750/950 nm, 750/415 nm, and 415/750 nm band ratios. The 750/950 nm ratio indicates FeO content — the deeper the absorption feature, the greater the FeO content. The other band ratios measure the "continuum slope" — the younger the soil, the flatter the slope. LOLA data yields topographic information at 100 m/pixel. LRO Narrow Angle Camera (NAC) images provide select, high resolution (0.5 m/pixel at 50 km altitude) panchromatic images of the lunar surface. NAC images were used when identification of small features and textures on scales of tens of meters was required to confirm unit characteristics or refine contact locations. Superposition, cross-cutting relations, and analysis of impact crater size-frequency distributions yielded relative and modeled absolute ages of map units, as well as chronostratigraphic ages for all impact craters > 2 km in diameter.

Geologic units: Units grouped by geographic setting include terra, plains, and basins. Terra units include ancient highlands (pNth), rugged terra of the SPA floor (pNtr), and knobby terra around Ingenii (pNtk). Smooth plains (pNps) are iron-enriched plains with a morphology potentially indicative of impact melt. Basin units (Nbr, pNbf, pNbr1, pNbr2) are associated with impact structures Poincaré, Planck, Ingenii, Leibnitz and Von Kármán.

Lithologic units include volcanic and impact categories. Volcanic products are primarily discrete, non-contiguous mare deposits occurring exclusively within, or breaching the rims of, craters or basins (smooth mare material; Ims). Mare composition is basaltic, similar to the nearside maria, but low in Fe and Ti. Mapped volcanic features include domes, wrinkle ridges, sinuous rilles and dark, Fe-rich plains (pNpd). Patches of smooth material enriched in FeO but buried or mixed into the regolith through impact activity (cryptomare [12]) are mapped as mantled mare (Nmm, Imm). Also present within some basins and craters are high-albedo, surficial swirl-like markings of the Reiner Gamma class (s).

Geologic History: The geologic record in the pre-Nectarian period was dominated by large impacts that formed Poincaré (~4.07 Ga), Planck (~4.06 Ga), Jules Verne (~4.01 Ga) and Von Kármán (~3.97 Ga) basins. The oldest terra units are the rugged and highlands terra (~4.06 Ga). The smooth plains unit (pNps) and iron-rich dark plains unit (pNpd) are also dated as pre-Nectarian, essentially contemporaneous with each other at ~4.00 and ~3.98 Ga respectively.

Key events during the Nectarian include formation of the Ingenii (~3.91 Ga) and Leibnitz (~3.88 Ga) basins, and the emplacement of mare within crater Hildegard. Crater statistics for all these areas are within, or nearly within, each other's error bars, suggesting that these events happened within at most a few tens of millions of years of each other. Ingenii ejecta would likely have covered most of the quadrangle, mantling any older mare deposits, if they existed [13].

Most volcanic deposits are late Imbrian. Larger ponds all cluster within ~3.74-3.71, except for one pond in Pauli crater (~3.61 Ga), and one in Poincaré F (~3.79 Ga). One possible interpretation based on the < 20 My of chronological separation of most mare ponds, is to consider all mare deposits as contemporaneous. However, the ponds in and around Poincaré were previously dated lower Imbrian by [8], and the two largest ponds in this area both pre-date all mare

deposits except for the oldest, likely less affected by Ingenii ejecta. These observations are consistent with an older age for the two deposits.

Changes from prior maps: The sequence of events derived from superposition and cross-cutting relations of geologic units are internally consistent with ages derived from cratering statistics; they also are consistent with the formation sequence of the larger craters and basins, as well as the general relationship between terra, plains and mare units. Also, results are consistent with an older age for knobby terra, dating it near the currently accepted date of the Imbrium impact, as noted by [6]. However, improved crater statistics yielded older dates for several craters previously dated as Eratosthenian or Copernican (O'Day, Pauli, ejecta mantling Leibnitz that derives from Finsen [6]). Additionally, statistics from the cratered highlands unit (which included degraded craters 25-100 km in diameter previously mapped as discrete structures and compositionally indistinguishable from their surroundings) yielded an age of 4.06 Ga +/- 0.00. The low dating error indicates these degraded craters are identical chronologically to nearby hills and mounds. Thus, fewer of these craters are mapped as discrete units.

Volcanic activity: The quadrangle is covered by ~3000-5000 km^2 more volcanic material than previously assessed [6-8]. A variety of features that are common products of effusive eruptions are observed (low-profile flow fronts, sinuous rilles). This result is consistent with the interpretation that effusive, highly-fluid eruptions were a common mode of volcanic emplacement on the farside. Additionally, the strong correlation of floor-fractured craters with spectrally fresh iron-bearing surface materials suggests a volcanic mechanism associated with fracturing, such as magmatic intrusion. These results indicate that the total volcanic budget, effusive and otherwise, is more spatially extensive and morphologically diverse (suggesting eruptive styles were also more diverse) than previously thought. Volcanic activity in the mapped region is extended in time as well; though the volcanic "production curve" is confirmed to have been greatest in the Late Imbrian, volcanism started earlier than previously thought, and lasted as long as previously assumed (no deposits subsequent to the Late Imbrian).

References: [1] Gaddis, L. (2002), *Abs. Annual Mtg. Planetary Mappers*, USGS Open-File Report 02-412. [2] Gaddis, L. et al. (2004) *Abs. Annual Mtg. Planetary Mappers*, USGS Open-File report 2004-1289. [3] Gaddis, L. et al. (2006) *Lunar Planet Sci. Conf*., *37th*, Abs. #2135. [4] Skinner, J. et al. (2006) *Abs. Annual Mtg. Planetary Mappers*, USGS Open-File Report 2006-1263. [5] Mest, S.C., and L.E. Van Arsdall (2008) NASA Lunar Science Institute Lunar Conference, 2089. [6] Stuart-Alexander, D. (1978) U.S. Geol. Surv. Map, I-1047. [7] Wilhelms, D. and F. El-Baz (1977) U.S. Geol. Surv. Map, I-948. [8] Wilhelms et al. (1979) U.S. Geol. Surv. Map, I-1162. [9] Smith, D. et al. (2010) *Space Sci. Rev.*, 150, 209–241. [10] Zuber, M. et al. (2010) *Space Sci. Rev.*, 150, 63–80. [11] Scholten, F. et al. (2012), *J. Geophys. Res*., *117*, E00H17. [12] Hawke, B.R. et al. (1990) LPI-LAPST Wksp on Mare Volcanism and Basalt Petrogenesis, p. 5-6. [13] Whitten, J. and J. Head (2015) *Icarus*, 247, 150-171.

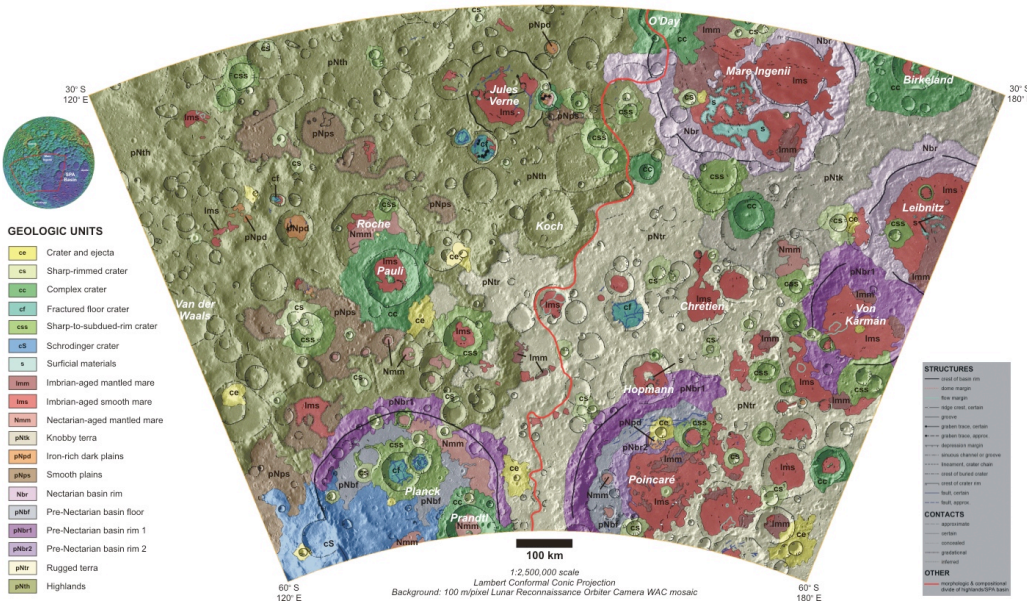

Figure 1. Geologic map of the lunar Planck Quadrangle (LQ-29).